Brachymesomelic Dysplasia With Peters Anomaly of the Eye Results From Disruptions of the X Chromosome Near the *SHOX* and *SOX3* Genes

Steven B. Bleyl,[1*] Janice L.B. Byrne,[2] Sarah T. South,[1] David C. Dries,[3] David A. Stevenson,[1] Alan F. Rope,[1] Angela M. Vianna-Morgante,[4] Gary C. Schoenwolf,[5] Jane D. Kivlin,[6] Arthur Brothman,[1] and John C. Carey[1]

[1]Department of Pediatrics, Division of Medical Genetics, University of Utah School of Medicine, Salt Lake City, Utah
[2]Department of Obstetrics and Gynecology, University of Utah School of Medicine, Salt Lake City, Utah
[3]Department of Ophthalmology, University of Utah School of Medicine, Salt Lake City, Utah
[4]Departamento de Genética e Biologia Evolutiva, Instituto de Biociências, Universidade de São Paulo, São Paulo, Brazil
[5]Department of Neurobiology and Anatomy, University of Utah School of Medicine, Salt Lake City, Utah
[6]Department of Ophthalmology, Medical College of Wisconsin, Milwaukee, Wisconsin

We report on a mother and son affected with an unusual skeletal dysplasia and anterior segment eye abnormalities. Their skeletal phenotype overlaps with the *SHOX*-related skeletal dysplasias and is intermediate between Leri–Weill dyschondrosteosis (LWD) and Langer Mesomelic dysplasia (LMD). The mother has bilateral Peters anomaly of the eye and was reported as having a new syndrome; the son had severe bilateral sclerocornea. Chromosome analysis showed that the mother has a pericentric inversion of the X chromosome [46,X,inv(X)(p22.3q27)] and the son, a resultant recombinant X chromosome [46,Y,rec(X)dup(Xq)inv(X)(p22.3q27)]. The observed skeletal and ophthalmologic abnormalities in both patients were similar in severity. The additional features of developmental delay, growth retardation, agenesis of the corpus callosum, cryptorchidism and hypoplastic scrotum in the son are consistent with Xq28 duplication. Analysis of the son's recombinant X chromosome showed that the Xp22.33 breakpoint lies 30–68 kb 5′ of the *SHOX* gene. This finding suggests that the skeletal dysplasia in both mother and son is allelic with LWD and LMD and results from a novel misexpression of *SHOX*. Analysis of the Xq27.1 breakpoint localized it to a 90 kb interval 3′ of the *SOX3* gene, supporting a novel role of *SOX3* misexpression in the development of Peters anomaly of the eye.
© 2007 Wiley-Liss, Inc.

Key words: Peters anomaly; sclerocornea; dyschondrosteosis; mesomelic dysplasia; X-chromosome inversion; *SHOX*; *SOX3*

INTRODUCTION

We previously reported on a patient with a unique mesomelic skeletal dysplasia and Peters anomaly of the eye [Kivlin et al., 1993]. At that time, this combination of findings had not been reported, and we proposed that this patient was affected with a provisionally unique genetic syndrome. To our knowledge, there have been no other reports of this condition. This patient subsequently had a son affected with strikingly similar skeletal and ophthalmologic abnormalities. He had additional congenital

anomalies that prompted high resolution chromosome analyses that showed a pericentric inversion of the X chromosome [46,X,inv(X)(p22.3q27)] in the mother and a recombinant X chromosome in the son [46,Y,rec(X)dup(Xq)inv(X)(p22.3q27)] with deletion of the Xp terminus and duplication of Xq27 → qter.

The skeletal anomalies seen in this mother and son overlap with, but are distinct from, those seen in Leri–Weill dyschondrosteosis (LWD) and Langer mesomelic dysplasis (LMD) and led to the hypothesis that the *SHOX* gene may be disrupted by the inversion. The short stature homeodomain (*SHOX*) gene is located in the pseudoautosomal regions of the short arms of the X and Y chromosomes and encodes a homeodomain protein thought to regulate the development of chondrocytes [Marchini et al., 2004]. Deletions and point mutations affecting the *SHOX* gene cause a range of skeletal abnormalities. Leri–Weill dyschondrosteosis (LWD [MIM 127300]) is a pseudoautosomal dominant disorder characterized by short stature, mesomelia and Madelung deformity. Approximately 65% of LWD is explained by heterozygous mutations of the *SHOX* gene [Belin et al., 1998; Shears et al., 1998; Schiller et al., 2000; Falcinelli et al., 2002; Flanagan et al., 2002] or by deletions of regions between 30 and 530 kb 3′ of the gene [Benito-Sanz et al., 2006]. These 3′ deletions may affect long-range *SHOX* regulatory elements. For about 35% of LWD patients the molecular defect has not been identified. Homozygous loss of *SHOX* has been demonstrated in Langer mesomelic dysplasia (LMD [MIM 249700]) [Belin et al., 1998]. LMD is characterized by more severe mesomelia with short square ulna, bowed radii, bowed tibia and hypoplastic fibulae [Langer, 1967]. Heterozygous mutations in the SHOX gene have also been described in 2–20% of patients with idiopathic short stature [Rao et al., 1997; Binder et al., 2000; Rappold et al., 2002; Stuppia et al., 2003; Huber and Cormier-Daire, 2004], and haploinsufficiency for *SHOX* is considered etiologically related to the short stature seen in Turner syndrome [Ellison et al., 1997; Rao et al., 1997; Clement-Jones et al., 2000].

Peters anomaly has not been described in association with SHOX-related disorders or other X-chromosome abnormalities, suggesting that the Xq27 breakpoint disrupts a novel gene involved in anterior segment abnormalities. Peters anomaly of the eye encompasses a range of abnormalities including corneal opacity, adherent iris strands and keratolenticular cataract. Peters anomaly is etiologically related to anterior segment mesodermal dysgenesis (ASMD), both abnormalities being caused by mutations in an overlapping set of genes. Mutations causing Peters anomaly and/or ASMD have been found in the genes encoding PAX6 [Jordan et al., 1992; Hanson et al., 1994], PITX2 [Semina et al., 1996; Doward et al., 1999], PITX3 [Semina et al., 1998], FOXC1 [Nishimura et al., 2001; Honkanen et al., 2003], FOXE3 [Semina et al., 2001; Valleix et al., 2006], EYA1 [Azuma et al., 2000], CYP1B1 [Stoilov et al., 1997], and FGFR2 [McCann et al., 2005]. Mutations in the gene encoding B3GALTL cause Peters-Plus syndrome [Lesnik Oberstein et al., 2006], an autosomal recessive condition characterized by anterior chamber defects and a primarily rhizomelic skeletal dsyplasia [Van Schooneveld et al., 1984]. Sclerocornea and aphakia are associated with microphthalmia and other anomalies in patients with mutations in the gene encoding SOX2 [Fantes et al., 2003; Ragge et al., 2005].

To better define the genetic etiology of the atypical pattern of dominantly inherited skeletal and ocular anomalies in mother and son, we undertook further studies to localize the breakpoints of the inversion and recombinant X chromosomes in these cases.

MATERIALS AND METHODS

Patients and Samples

Blood was collected with informed consent and approval from the University of Utah Institutional Review Board (IRB) protocol number 7551.

Chromosome Analysis

High-resolution G-banded karyotype analysis was performed on peripheral lymphocytes using standard techniques. Fluorescence in situ hybridization (FISH) was performed using subtelomeric probes for the Xp/Yp and Xq/Yq regions (Vysis, Downers Grove, IL), and with BAC RP11-839D20 (Spectral Genomics, Houston, TX), by standard methods.

Comparative Genomic Hybridization Analysis

Array comparative genomic hybridization (aCGH) analysis was performed using the 1 Mb average resolution SpectralChip 2600 (Spectral Genomics), according to the manufacturer's protocol. Scanning was performed with Axon's GenePix 400B microarray scanner and the images were analyzed with SpectralWare 2.0 (Spectral Genomics) for the preparation of ratio plots. For high-resolution CGH, chip 8 of the 8-array Set with an average of 713 bp probe spacing was performed by the manufacturer, and relative ratios (RRs) were determined using the SignalMap software package, version 1.8 (NimbleGen Systems, Madison, WI).

Quantitative Real-Time PCR

Custom TaqMan gene probes for five loci spanning the deletion boundary and for exons 1 and 23 of the *PDGFRA* gene at 4q12 (used as controls) were designed by ABI (Applied Biosystems, Foster City,

CA). Primer and probe sequences were as follows: P1For: TGCTGGCCTCGCTGAG. P1Rev: CCGGTC-CTGAAGATGAAGGT. P1Fam: CCAGTACAGGAA-CAGCTC. M1For: GGTGCTCAGAGCCTCTAGGA. M1Rev: CATTAAATGAGCGTCCTCCAACTC. M1Fam: TTTCGGAAAGCAAGTCTG. M2For: CATTGCATGT-AATCGGCACTTCATT. M2Rev: GTGTGCAGAA-GCCCTAGCT. M2Fam: CCACTGCCTGTAACTAA. M3For: GGAGCCCACTTTCTTGCTTTTAAAT. M3Rev: CTGCAGAGGAAGACGAGTTATGTC. M3Fam: TT-CCAGCCCCAACCCT. S5′For: CCCCCAGGAGCCAA-TAGG. S5′Rev: TCAGGACCCGGGCAAAAG. S5′FAM: CCCTGCGGCCGCCTG. Genomic DNA was combined with TaqMan probes and Universal master mix and analyzed on an ABI 7900HT RT-PCR system, according to manufacturer specifications. Patient and control reactions were done in triplicate and threshold cycle (Ct) measurements were averaged. RRs were calculated using the $\Delta\Delta Ct$ method [Livak and Schmittgen, 2001].

X-Inactivation Studies

The pattern of X-inactivation was determined in the mother's lymphocytes based on the methylation status of HpaII restriction-enzyme sites closely linked to the polymorphic CAG repeat in the human androgen-receptor (AR) gene, as previously described [Allen et al., 1992].

In Silico Analysis

The March 2006 assembly of the UCSC Human Genome (http://www.genome.ucsc.edu) was used as the primary tool to map probes and genes to genomic sequence. Alignment of deleted probes to the known genomic region surrounding breakpoints was performed using the Sequencher (version 4.5) software package (Gene Codes, Corp. Ann Arbor, MI). Alignment of genomic sequences surrounding the breakpoints to each other was performed using the NCBI BLAST 2 sequences tool (http://www.ncbi.nlm.nih.gov:80/BLAST/).

RESULTS

Clinical Reports

The proband (mother) was described previously [Kivlin et al., 1993]. Briefly, she was a full-term infant with a birth weight of 2,880 g (−1.0 SD), OFC 36.5 cm (+1.0 SD), length 45.5 cm (−1.7 SD). Shown in Figure 1A, she had minor variation in the shape of her ears with a flat forehead and double hair whorls, but a normal jaw. Distal limbs were short and limited extension of the elbow to 150° with ulnar deviation of the wrists was noted. There was camptodactyly of the 4th fingers and rotation of the 5th finger toward the palm bilaterally. The lower limbs showed decreased muscle mass and reduced extension of the knees to 160°. She had bilateral hip dislocation and talipes equinovarus with cavus deformities.

Radiographs of the upper extremities (Fig. 1C) showed short, bowed radii and markedly short, thickened ulnae. Lower extremity films (Fig. 1E) showed shortening of the tibiae and fibulae, but to a lesser degree, without fibular hypoplasia. Her ocular anomalies consisted of bilateral corneal clouding that was more severe on the left (Fig. 2A) with bilateral anterior iris synechiae and absence of Decemet's membrane seen on histological exam of the left cornea after transplantation (Fig. 2C).

The proband was seen again at age 20 years then pregnant at 19 weeks gestation. She was 124.5 cm height and blind in her left eye (after two corneal transplants). She was ambulatory over short distances, but relied heavily on assistive devices, including an electric wheelchair. She was developmentally normal, although she had required some resource classes in school. Her partner was of low normal height, with normal extremities. He was affected with Neurofibromatosis type 1 and had mild learning disabilities.

Ultrasound examination of the fetus at 19 weeks revealed lower normal length femora and humeri, short distal extremities, bilateral talipes equinovarus and bilateral ulnar deviation of the hands, consistent with a recurrence of the mother's skeletal dysplasia in the fetus. By 25 weeks of gestation, all long bones except the humeri were short (3–6 SD below the mean), and the radii and ulnae were thickened and curved. The pregnancy was otherwise uncomplicated.

At 38.5 weeks of gestation, the infant was delivered by primary cesarean for inadequate maternal pelvis. The male infant weighed 2,335 g (−1.9 SD). His length was 36 cm (<−3.3 SD). His OFC was 32 cm (−1.7 SD). Similar to his mother, he had brachymesomelic shortening of his extremities, knee contractures, bilateral clubfeet, camptodactyly and ulnar deviation of his wrists. Additionally he had undescended testes, a hypoplastic scrotum, and agenesis of the corpus callosum. There was one café au lait spot on the abdomen, but no other neurocutaneous stigmata. He had significant feeding problems, constipation and severe gastroesophageal reflux, requiring a nissen funduplication and gastrostomy tube placement. Despite these measures, he continued to have persistent severe growth retardation with a weight of 4.5 kg, an OFC of 42 cm and a length of 48 cm (all well below the 3rd centile) at 15 months of age. Cognitive development was also significantly delayed. He smiled at 6 months of age, but never rolled or sat without support. Although visually impaired, he was interactive and would play, but had no words at 22 months of age. Echocardiography, renal ultrasound and thyroid function studies
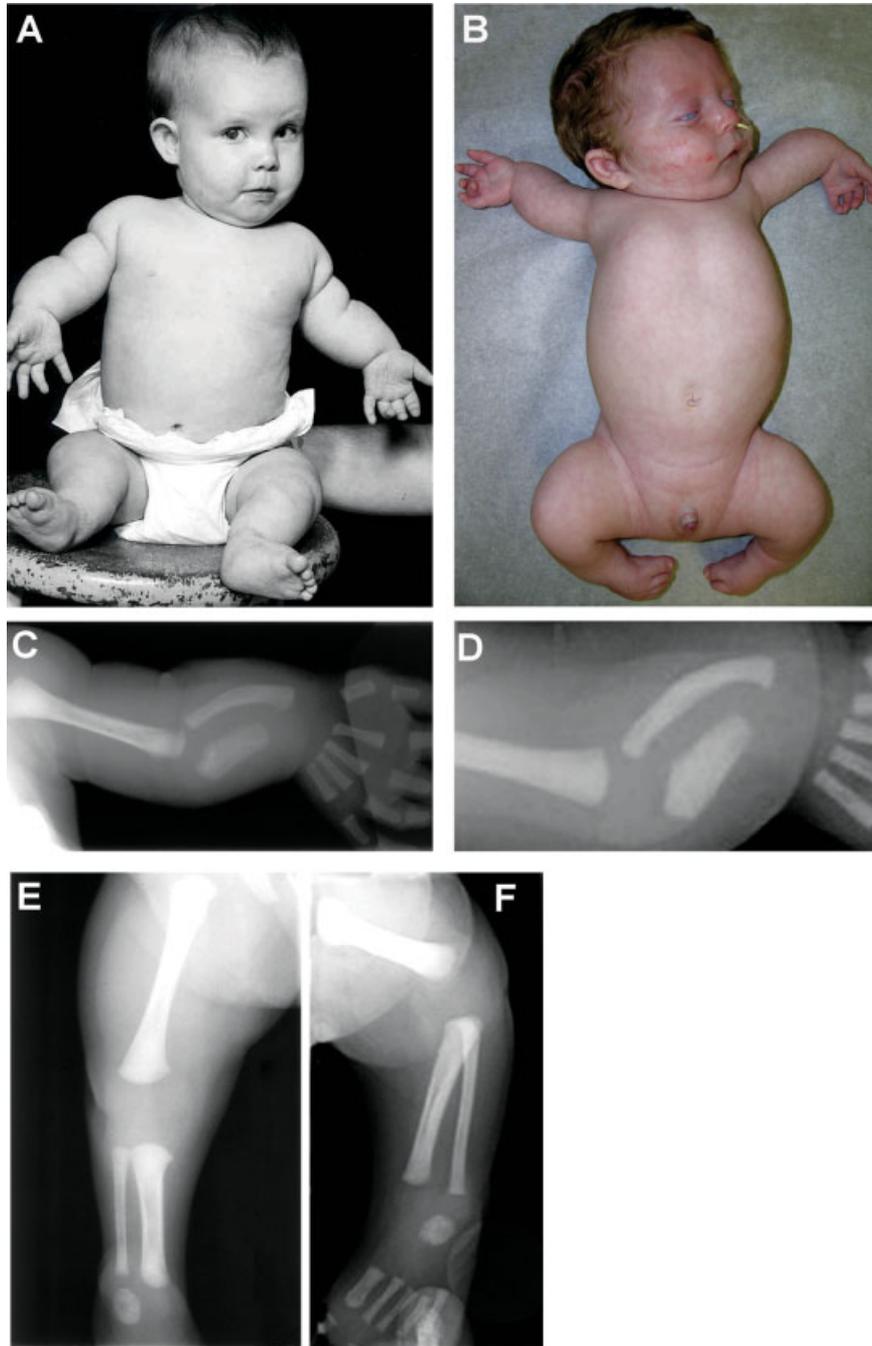
Fig. 1. Skeletal phenotypes in the mother (**A,C,E**) and son (**B,D,F**) showing mesomelic shortening of the upper and lower limbs. Left upper extremity radiographs (C,D) show similar short, square ulnae, and bowed radii in both patients. Lower extremity films (E,F) show mesomelic shortening without bowing of the tibiae or hypoplasia of the fibulae.

were all normal. The patient went on to have a complicated medical course with an acute presentation of sepsis and bowel necrosis, requiring total colectomy at 22 months. He had recurrent fevers and required treatment for septic shock. He had multiple respiratory infections with chronic lung disease. He eventually succumbed to these complex medical issues at 22.5 months of age.

His radiographic findings were nearly identical to those of his mother as an infant (Fig. 1D,F). Ocular examination showed complete bilateral sclerocornea (Fig. 2B) with formed anterior chambers and no iris-corneal adhesions by ultrasound biomicroscopy (Fig. 2D). No evidence for microphthalmia was observed. The axial length of the eyes was 22.0 mm OD and 21.7 mm OS.
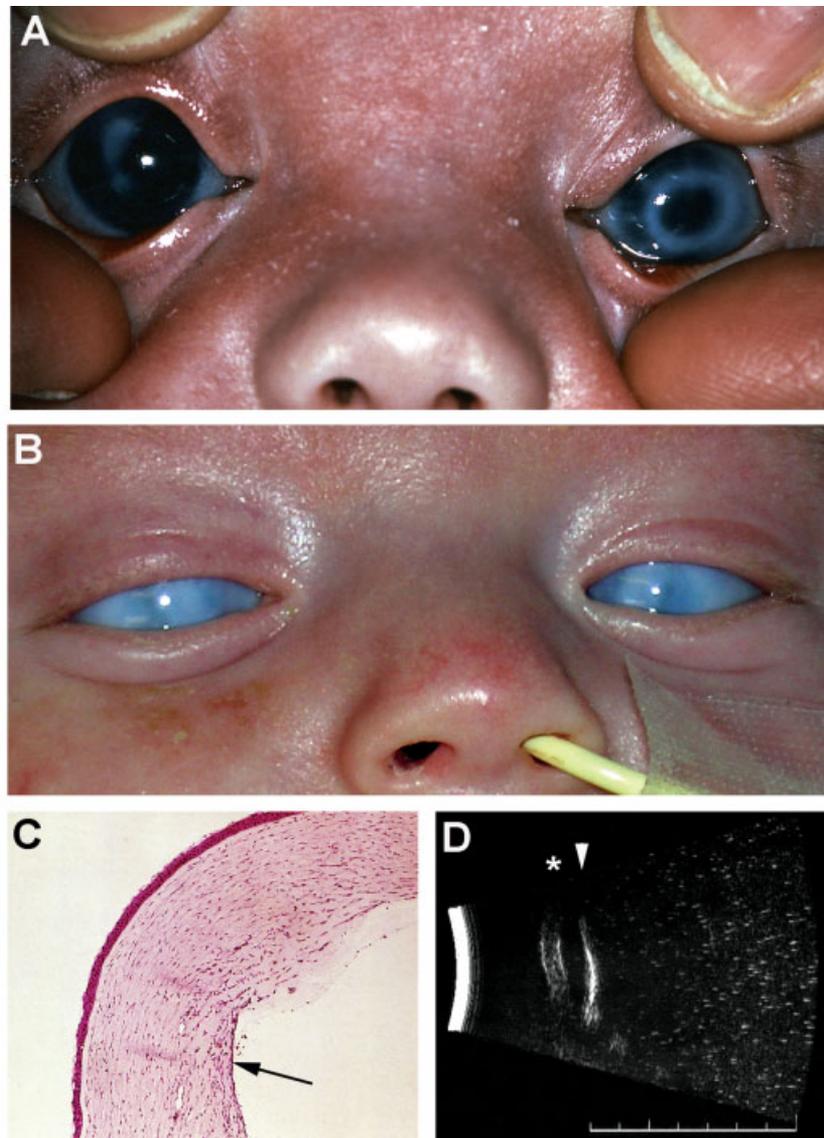
FIG. 2. External ocular findings in the mother (**A**) showed bilateral corneal clouding that was worse in the left eye. The son (**B**) had severe bilateral sclerocornea. Histological section through the mother's left cornea (**C**) following corneal transplantation showed hypercellular stroma and an area of complete absence of Decemet's membrane (arrow) diagnostic of Peters anomaly. Ultrasound biomicroscopy (**D**) of the son's eye did not detect lens abnormalities or iris-corneal adhesions. For reference, an asterisk is directly above the cornea and an arrowhead is above the iris.

Chromosome Analyses

The similar presentation of skeletal dysplasia and anterior chamber eye anomalies seen in both mother and son suggested a new autosomal dominant syndrome. However, based on the presence of additional multiple congenital anomalies in the son, chromosome analyses were performed that revealed a large pericentric inversion of the X chromosome in the mother [46,X,inv(X)(p22.3q27)] and a resultant recombinant X chromosome [46,Y,rec(X)dup(Xq)inv(X)(p22.3q27)] in the son (Fig. 3A). The inversion in the mother was found to be de novo based on normal cytogenetic studies

done in her parents. FISH was performed using probes from the Xp/Yp and the Xq/Yq subtelomeric regions. Both Xp and Xq probes hybridized to the normal and inverted X chromosomes in the mother (Fig. 3B). On the son's recombinant chromosome, FISH showed absence of the Xp probe signal (Fig. 3C), and presence of Xq signals on both ends (Fig. 3D), thus documenting a deletion of distal Xp and disomy for distal Xq.

Comparative Genomic Hybridization

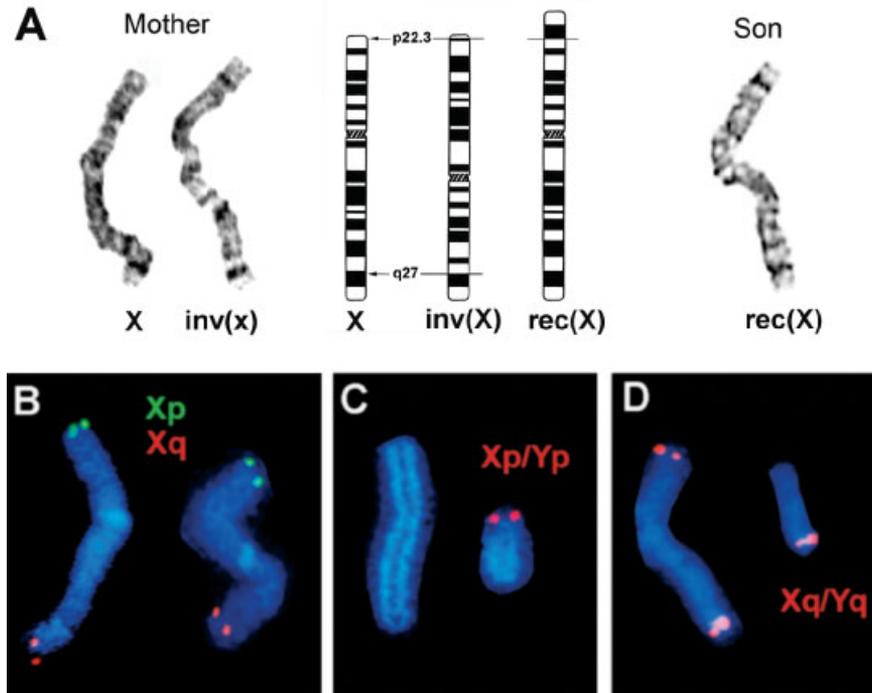We performed aCGH to investigate the possibility of cryptic copy number changes near the breakpoints

Fɪɢ. 3. **A**: High-resolution chromosome banding (650-band level) analysis of the mother revealed a pericentric inversion of the X chromosome (left) with breakpoints in distal Xp and Xq. The son carried a recombinant X chromosome (right) with deletion of Xp and partial duplication of Xq. Ideograms of the three X chromosomes are shown (center) with arrows marking breakpoints in Xp23.3 and Xq27. FISH in the mother using subtelomeric probes confirmed the presence of both Xpter and Xqter (**B**) and the deletion of Xpter (**C**), and duplication of the Xqter (**D**) in the son.

of the mother's inversion, and to better characterize the extent of gains and losses on the son's recombinant X chromosome. Using the 1 Mb Spectral Genomics array, no gains or losses were detected on the mother's X chromosome near the inversion breakpoints. The son's analysis showed a single terminal clone (RP11-839D20) deletion at Xp22.33, and a 12-clone duplication in the Xq27-28 interval. This array mapped the Xp22.33 and Xq27 breakpoints to 5.4 and 7 Mb intervals, respectively.

Next, to map the Xq27.1 breakpoint with higher resolution, aCGH was performed using chip 8 of the 8-chip NimbleGen 713 bp array. The Xp22.33 pseudoautosomal region was omitted from this chip. This analysis localized the Xq27.1 breakpoint to a 13 kb interval that lies 92 kb centromeric of the *SOX3* gene (Fig. 4) within a cluster of LINE elements. The *SOX3* gene is oriented such that the breakpoint lies 3′ of the gene.

Quantitative Real-Time PCR

The aCGH analysis mapped the Xp22.33 breakpoint to a large interval of 5.4 Mb that contains the *SHOX* gene (Fig. 5), which is mutated in two skeletal dysplasia syndromes with overlap to the phenotypes seen in our patients. To determine if the *SHOX* gene was disrupted by the inversion breakpoint in the mother or deleted in the son, quantitative real-time PCR (RT-PCR) was used. TaqMan RT-PCR

probes were designed at five sites across the interval (Fig. 5A), including a probe within RP11-839D20, known to be deleted by aCGH analysis, and a probe at the 5′ end of the *SHOX* gene. TaqMan probes for two loci at 4q12 were used as controls. The analysis showed that three probes were deleted in the son, but that the 5′ end of the *SHOX* gene was not disrupted. A representative amplification plot is shown in Figure 5B. The same analysis found no deleted probes in the mother. The inversion breakpoint was mapped to the 34 kb interval that lies 33–68 kb distal to the *SHOX* gene (Fig. 5A).

X-Inactivation Studies

The similarity of skeletal and ocular phenotypes in mother and son raised the possibility of skewed X-inactivation in the mother. X-inactivation studies showed a partially skewed pattern of inactivation, and the *AR* allele, found to be active on about 75% of the mother's X chromosomes, was the allele inherited by her son on the recombinant chromosome (data not shown). However, we could not determine whether this allele was present on the inverted chromosome in the mother.

Breakpoint Analysis

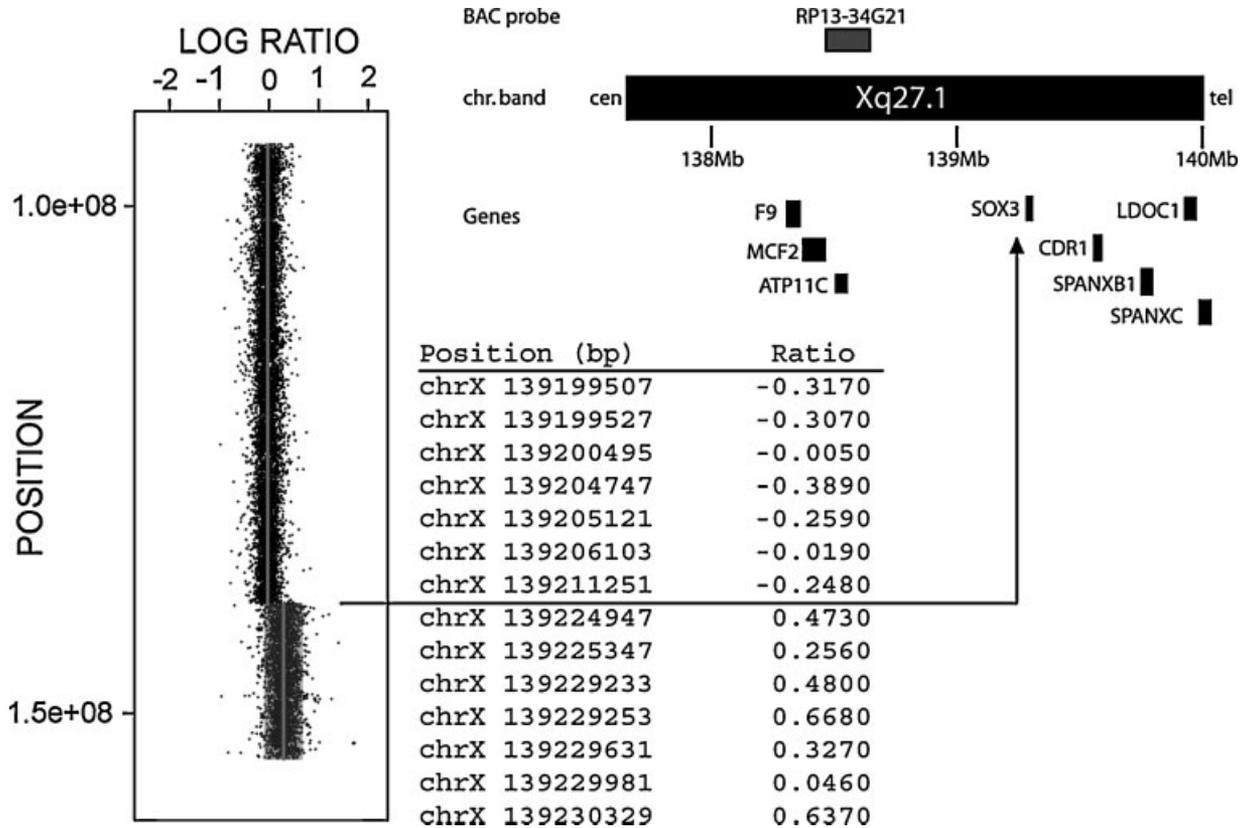The Xq27.1 breakpoint occurs within a 13 kb LINE element cluster, but no homologous LINE elements

FIG. 4. High-resolution aCGH mapped the Xq27.1 breakpoint to a 13.6 kb interval that lies about 90 kb proximal to the SOX3 gene (arrow). A shift in ratios plots (from near 0 to near 0.5 indicating a duplication) is seen between probes at 139,211,251 and 139,224,947 bp of the X chromosome sequence.

were found near the Xp22.33 breakpoint in the UCSC browser. Sequence homology has been observed near the breakpoints of recurrent intrachromosomal rearrangements. However, BLAST alignment of 100 kb segments flanking each breakpoint revealed no sequence identity greater than 1 kb in length.

DISCUSSION

We describe a mother and son with a strikingly similar syndrome of mesomelic skeletal dysplasia and abnormalities of the anterior segment of the eye associated with disruptions of the X chromosome. The mother's case was previously reported as a new syndrome [Kivlin et al., 1993]. The differential diagnosis of the mother's condition, as discussed in our previous report prior to the discovery of her X chromosome inversion, included Peters plus syndrome, acromesomelic dysplasia and LMD. However, the discovery of X chromosome abnormalities in these individuals with overlapping skeletal and ocular findings would strongly suggest an X-linked etiology. Mapping of the Xp22.3 and Xq27 breakpoints in these cases suggests a role for the SHOX gene in the skeletal dysplasia and for the SOX3 gene in the ocular anomalies, respectively. The findings of

severe mesomelic shortening preferentially affecting the upper extremities with short square ulnae and severely angulated radii in our patients resemble the upper extremity findings in LMD. LMD is caused by pseudoautosomal recessive loss of the SHOX gene and presents with severe mesomelia of the lower limbs with hypoplastic fibulae and curved tibia. Our patients have less severe lower extremity defects, and also lack the severe rhizomelia often seen in LMD. Without sequencing the SHOX genes present on the normal X (in the mother) and Y (in the son) chromosomes, we cannot be certain that their skeletal phenotype does not represent a variant form of the recessive LMD. However, this possibility would require that both mother and son inherited additional SHOX mutations from each of their unrelated fathers who had normal height and normal limbs. We view this as an extremely unlikely explanation. Disruption of just one copy of SHOX would predict a phenotype resembling the pseudoautosomal dominant Leri–Weil dyschondrosteosis (LWD). LWD presents with short stature and milder mesomelia of the upper extremities and Madelung deformity. The novel skeletal phenotypes seen in these patients, which affect the upper extremities preferentially like LWD yet lies closer in
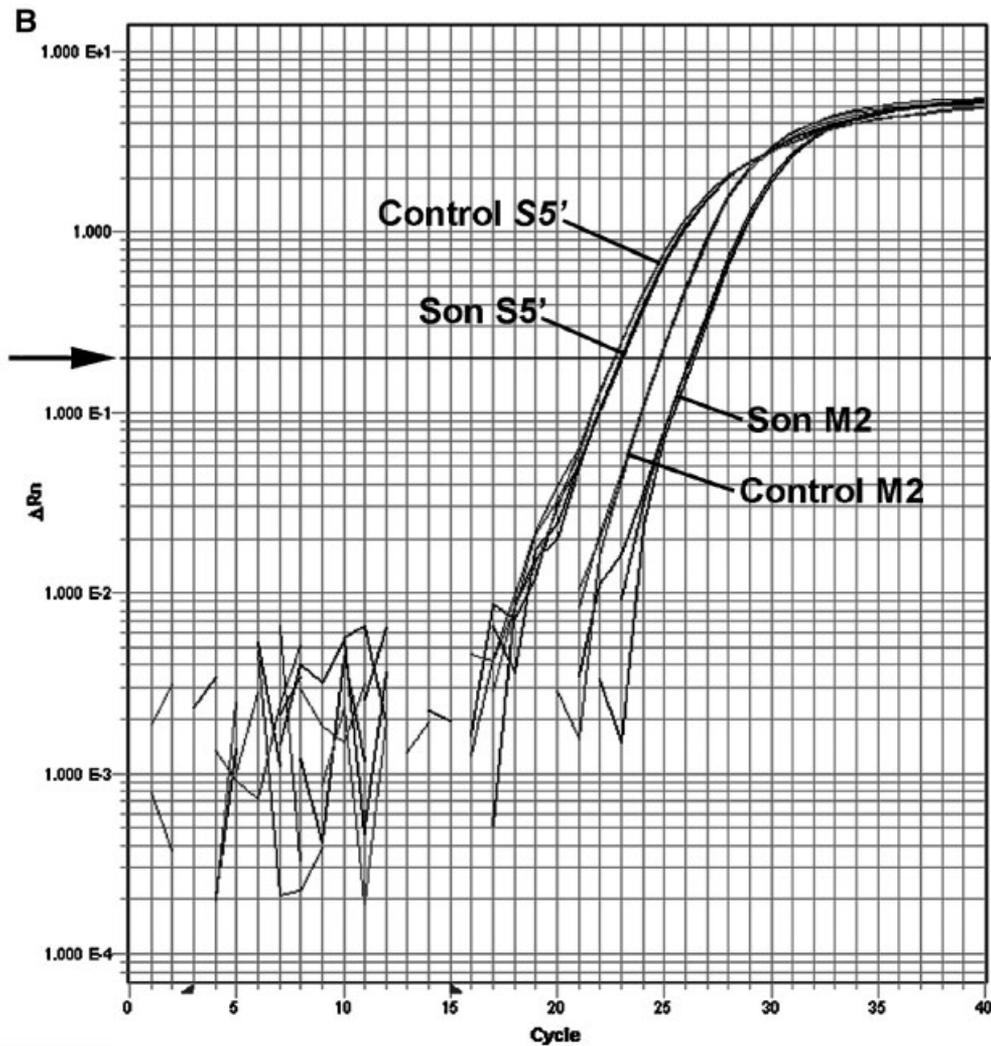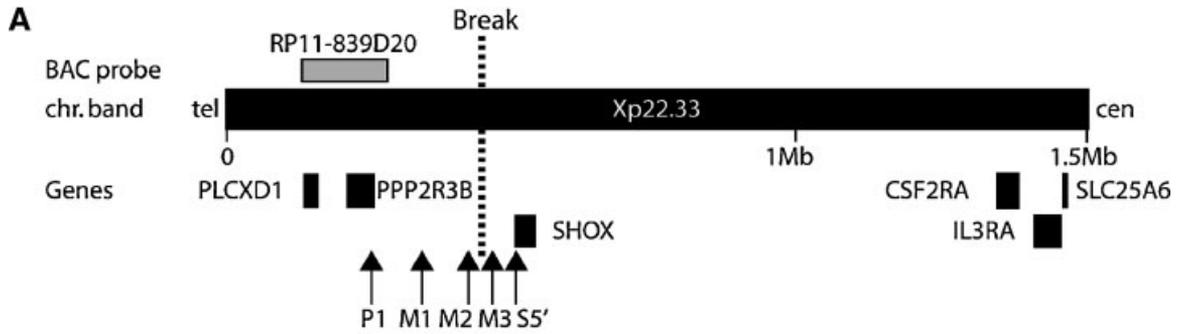
FIG. 5. **A**: A map of Xp22.33 showing all known genes located within1.5 Mb from the Xpter. aCGH in the son showed deletion of a single BAC clone (RP11-839D20) that lies 240 kb distal to the *SHOX* gene. Five RT-PCR probes (P1, M1, M2, M3, S5′) were designed spanning the interval between this BAC and the *SHOX* gene. **B**: Plot comparing real-time amplification of control and patient (the son) DNA using probe S5′ (left) and probe M2 (right). Amplification of the patient DNA with the M2 probe reaches the threshold (arrow) at roughly one cycle count later than the control DNA relative to amplification of the S5′ probe (at the 5′ end of *SHOX*). Control S5′ Ct = 22.48; control M2 Ct = 24.57; patient S5′ Ct = 22.98; patient M2 Ct = 26.30. The relative ratio (RR) calculated using these Ct values is 0.43 indicating a deletion of the M2 probe in the DNA sample from the patient relative to the *SHOX* 5′ probe. The analysis showed that three probes were deleted in the son (RR = 0.41, 0.50, and 0.43 for the P1, M1, and M2 probes, respectively, normalized to a control probe and compared to a random control individual), but that the 5′ end of the *SHOX* gene was not disrupted (RR = 1.08 and 0.99 for the M3 and S5′ probes, respectively).

severity to LMD, could suggest a novel disruption of the *SHOX* gene. Our finding that the coding region of the *SHOX* gene is, in fact, not disrupted, supports the hypothesis that misexpression of *SHOX*, due to a position effect, underlies this skeletal dysplasia. Our findings also suggest that this brachymesomelic skeletal dysplasia is allelic with LWD and LMD, as well as the other *SHOX*-related skeletal disorders including idiopathic short stature and the short stature of Turner syndrome. Finally, disruption upstream of the *SHOX* gene could explain a portion of LWD cases in which *SHOX* coding region mutations are not found, particularly those cases with more severe upper extremity involvement.

SHOX misexpression in these cases could involve either reduced expression due to loss of 5′ enhancers or ectopic expression due to gain of inappropriate enhancers or due to loss of *SHOX* repressors remains a possibility. The regulatory elements controlling *SHOX* expression have not been elucidated, but precedence for long-range regulation of the gene exists. Benito-Sanz et al. [2006] reported patients with LWD who harbor deletions in the 3′ region of the gene as far as 500 kb away. Precedence for overexpression causing defects preferentially in the upper extremities exists, as well, in the report by Grigelioniene et al. [2001], who described one patient with severe isolated Madelung deformity and a tandem duplication of the SHOX gene. However, disruptions 5′ of the *SHOX* gene associated with skeletal phenotypes have not been reported.

Peters anomaly of the eye and bilateral severe scelerocornea have not been reported with *SHOX*-related disorders. Peters anomaly of the eye and sclerocornea are related conditions in the spectrum of ASMD. Because ASMD is often associated with microphthalmia/anophthalmia (although not in this family), we considered the various loci for microphthalmia located on the X-chromosome as potentially causative. Two Xp-linked syndromes with ocular abnormalities include microphthalmia with linear skin defects (MLSD; MIM 300166), which involves more proximal Xp deletions at Xp22.31, and microphthalmia, cataracts, radiculomegaly and septal heart defects (MCOPS2; MIM 309801) that is caused by mutations in the *BCOR* gene at Xp11.4. Two Xq-linked ocular disorders, Lenz microphthalmia (MCOP1; MIM 309800) and ANOP1 (MCOP4; MIM 301590), map to Xq27-28 but lie distal to the breakpoint in our patients. This lack of association between X chromosome abnormalities and anterior chambers defects suggested the possibility that a novel gene for Peters anomaly was disrupted at Xq27.1 in our patients. However, it is formally possible that the mother in this case harbors a mutation in one of the genes known to cause Peters anomaly (e.g., *PAX6*), which she also passed to her affected son, independent of their X-chromosome abnormalities. Sequencing of Peters anomaly genes has not been done.

Mapping of the Xq27.1 breakpoint by aCGH localized the breakpoint in these cases to an interval that lies approximately 90 kb 3′ of the *SOX3* gene. No other genes lie within 350 kb. Deletions, duplications and point mutations of the *SOX3* gene have all been reported and cause X-linked hypopituitarism with or without mental retardation [Laumonnier et al., 2002; Woods et al., 2005]. A large deletion-insertion occurring 67 kb downstream of the *SOX3* gene is associated with X-linked recessive hypoparathyroidism in males [Bowl et al., 2005]. The patients in these reports had no ocular anomalies. However, disruptions of the closely related *SOX2* gene are associated with anterior segment anomalies and microphthalmia [Fantes et al., 2003; Ragge et al., 2005]. Further, misexpression of *Sox2* in the developing eyes of chick embryos causes abnormalities of the anterior chamber, and *Sox2* and *Sox3* are functionally similar in their ability to activate lens-specific genes like *δ-crystallin* [Kamachi et al., 2001; Kondoh et al., 2004]. Therefore, we hypothesize that misexpressed *SOX3* could have led to the anterior chamber abnormalities in these patients, again due to a position effect.

The mother had partially skewed X-inactivation in lymphocytes. The *SHOX* gene is pseudoautosomal, and therefore X-inactivation is irrelevant for the phenotype resulting from its altered expression. On the other hand, the *SOX3* gene is subject to inactivation, and both mother and son have a normal copy of this gene, present on the mother's normal X and on the duplicated segment of the recombinant chromosome in the son. Partially skewed X-inactivation in the mother may have contributed to the similarity between her clinical manifestations and those of her son, assuming that the altered allele is in the more frequently active X chromosome.

Blast analysis comparing the breakpoints in this mother and son revealed no homologous repeat DNA to explain the mechanism of inversion. The Xq27.1 breakpoint did occur within a 13 kb LINE element cluster. However, this breakpoint region appears to be distinct from those reported in other disruptions near the *SOX3* gene [Bowl et al., 2005; Woods et al., 2005].

In summary, our identification of X chromosome disruptions in this mother and son redefines this syndrome of brachymesomelic skeletal dysplasia with Peters anomaly of the eye. The breakpoints involved lie near genes plausibly related to the observed spectrum of defects (Fig. 6), leading us to speculate that misexpression of both *SHOX* and *SOX3*, due to position effects, causes the observed skeletal and ocular abnormalities, respectively. Analysis of these genes in patients with either similar skeletal dysplasias, or anterior segment ocular abnormalities, may confirm this hypothesis.
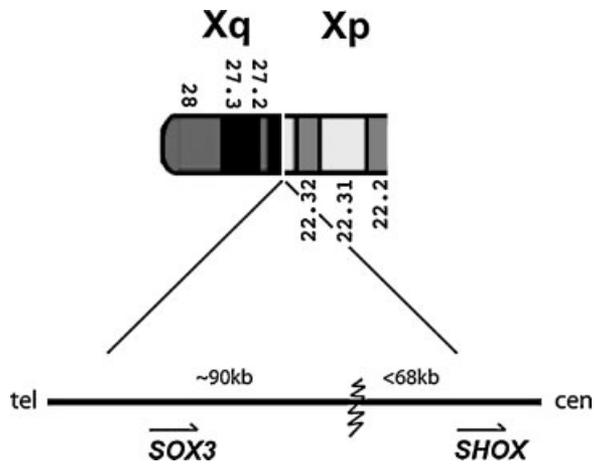
FIG. 6. A schematic representation of the Xq and Xp breakpoints and fusion present in the rearranged X chromosomes of both mother (inversion X) and son (recombinant X), with the *SOX3* and *SHOX* genes positioned in a head-to-tail configuration and lying approximately 160 kb apart.

In particular, we put forward the *SOX3* gene as a possible candidate gene for isolated Peters anomaly and other anterior segment ocular abnormalities.

ACKNOWLEDGMENTS

REFERENCES

Allen RC, Zoghbi HY, Moseley AB, Rosenblatt HM, Belmont JW. 1992. Methylation of HpaII and HhaI sites near the polymorphic CAG repeat in the human androgen-receptor gene correlates with X chromosome inactivation. Am J Hum Genet 51:1229–1239.

Azuma N, Hirakiyama A, Inoue T, Asaka A, Yamada M. 2000. Mutations of a human homologue of the Drosophila eyes absent gene (EYA1) detected in patients with congenital cataracts and ocular anterior segment anomalies. Hum Mol Genet 9:363–366.

Belin V, Cusin V, Viot G, Girlich D, Toutain A, Moncla A, Vekemans M, Le Merrer M, Munnich A, Cormier-Daire V. 1998. SHOX mutations in dyschondrosteosis (Leri-Weill syndrome). Nat Genet 19:67–69.

Benito-Sanz S, del Blanco DG, Aza-Carmona M, Magano LF, Lapunzina P, Argente J, Campos-Barros A, Heath KE. 2006. PAR1 deletions downstream of SHOX are the most frequent defect in a Spanish cohort of Leri-Weill dyschondrosteosis (LWD) probands. Hum Mutat 27:1062.

Binder G, Schwarze CP, Ranke MB. 2000. Identification of short stature caused by SHOX defects and therapeutic effect of recombinant human growth hormone. J Clin Endocrinol Metab 85:245–2249.

Bowl MR, Nesbit MA, Harding B, Levy E, Jefferson A, Volpi E, Rizzoti K, Lovell-Badge R, Schlessinger D, Whyte MP, Thakker RV. 2005. An interstitial deletion-insertion involving chromo-somes 2p25.3 and Xq27.1, near SOX3, causes X-linked recessive hypoparathyroidism. J Clin Invest 115:2822–2831.

Clement-Jones M, Schiller S, Rao E, Blaschke RJ, Zuniga A, Zeller R, Robson SC, Binder G, Glass I, Strachan T, Lindsay S, Rappold GA. 2000. The short stature homeobox gene SHOX is involved in skeletal abnormalities in Turner syndrome. Hum Mol Genet 9:695–702.

Doward W, Perveen R, Lloyd IC, Ridgway AE, Wilson L, Black GC. 1999. A mutation in the RIEG1 gene associated with Peters' anomaly. J Med Genet 36:152–155.

Ellison JW, Wardak Z, Young MF, Gehron Robey P, Laig-Webster M, Chiong W. 1997. PHOG, a candidate gene for involvement in the short stature of Turner syndrome. Hum Mol Genet 6:1341–1347.

Falcinelli C, Iughetti L, Percesepe A, Calabrese G, Chiarelli F, Cisternino M, De Sanctis L, Pucarelli I, Radetti G, Wasniewska M, Weber G, Stuppia L, Bernasconi S, Forabosco A. 2002. SHOX point mutations and deletions in Leri-Weill dyschondrosteosis. J Med Genet 39:E33.

Fantes J, Ragge NK, Lynch SA, McGill NI, Collin JR, Howard-Peebles PN, Hayward C, Vivian AJ, Williamson K, van Heyningen V, FitzPatrick DR. 2003. Mutations in SOX2 cause anophthalmia. Nat Genet 33:461–463.

Flanagan SF, Munns CF, Hayes M, Williams B, Berry M, Vickers D, Rao E, Rappold GA, Batch JA, Hyland VJ, Glass IA. 2002. Prevalence of mutations in the short stature homeobox containing gene (SHOX) in Madelung deformity of childhood. J Med Genet 39:758–763.

Grigelioniene G, Schoumans J, Neumeyer L, Ivarsson A, Eklof O, Enkvist O, Tordai P, Fosdal I, Myhre AG, Westphal O, Nilsson NO, Elfving M, Ellis I, Anderlid BM, Fransson I, Tapia-Paez I, Nordenskjold M, Hagenas L, Dumanski JP. 2001. Analysis of short stature homeobox-containing gene (SHOX) and auxological phenotype in dyschondrosteosis and isolated Madelung deformity. Hum Genet 109:551–558.

Hanson IM, Fletcher JM, Jordan T, Brown A, Taylor D, Adams RJ, Punnett HH, van Heyningen V. 1994. Mutations at the PAX6 locus are found in heterogeneous anterior segment malformations including Peters' anomaly. Nat Genet 6:168–173.

Honkanen RA, Nishimura DY, Swiderski RE, Bennett SR, Hong S, Kwon YH, Stone EM, Sheffield VC, Alward WL. 2003. A family with Axenfeld-Rieger syndrome and Peters Anomaly caused by a point mutation (Phe112Ser) in the FOXC1 gene. Am J Ophthalmol 135:368–375.

Huber C, Cormier-Daire V. 2004. [Genetics and the SHOX gene]. Arch Pediatr 11:555–556.

Jordan T, Hanson I, Zaletayev D, Hodgson S, Prosser J, Seawright A, Hastie N, van Heyningen V. 1992. The human PAX6 gene is mutated in two patients with aniridia. Nat Genet 1:328–332.

Kamachi Y, Uchikawa M, Tanouchi A, Sekido R, Kondoh H. 2001. Pax6 and SOX2 form a co-DNA-binding partner complex that regulates initiation of lens development. Genes Dev 15:1272–1286.

Kivlin JD, Carey JC, Richey MA. 1993. Brachymesomelia and Peters anomaly: A new syndrome. Am J Med Genet 45:416–419.

Kondoh H, Uchikawa M, Kamachi Y. 2004. Interplay of Pax6 and SOX2 in lens development as a paradigm of genetic switch mechanisms for cell differentiation. Int J Dev Biol 48:819–827.

Langer LO Jr. 1967. Mesomelic dwarfism of the hypoplastic ulna, fibula, mandible type. Radiology 89:654–660.

Laumonnier F, Ronce N, Hamel BC, Thomas P, Lespinasse J, Raynaud M, Paringaux C, Van Bokhoven H, Kalscheuer V, Fryns JP, Chelly J, Moraine C, Briault S. 2002. Transcription factor SOX3 is involved in X-linked mental retardation with growth hormone deficiency. Am J Hum Genet 71:1450–1455.

Lesnik Oberstein SA, Kriek M, White SJ, Kalf ME, Szuhai K, den Dunnen JT, Breuning MH, Hennekam RC. 2006. Peters Plus syndrome is caused by mutations in B3GALTL, a putative glycosyltransferase. Am J Hum Genet 79:562–566.

Livak KJ, Schmittgen TD. 2001. Analysis of relative gene expression data using real-time quantitative PCR and the 2(-Delta Delta C(T)) method. Methods 25:402–408.

Marchini A, Marttila T, Winter A, Caldeira S, Malanchi I, Blaschke RJ, Hacker B, Rao E, Karperien M, Wit JM, Richter W, Tommasino M, Rappold GA. 2004. The short stature homeodomain protein SHOX induces cellular growth arrest and apoptosis and is expressed in human growth plate chondrocytes. J Biol Chem 279:37103–37114.

McCann E, Kaye SB, Newman W, Norbury G, Black GC, Ellis IH. 2005. Novel phenotype of craniosynostosis and ocular anterior chamber dysgenesis with a fibroblast growth factor receptor 2 mutation. Am J Med Genet Part A 138A:278–281.

Nishimura DY, Searby CC, Alward WL, Walton D, Craig JE, Mackey DA, Kawase K, Kanis AB, Patil SR, Stone EM, Sheffield VC. 2001. A spectrum of FOXC1 mutations suggests gene dosage as a mechanism for developmental defects of the anterior chamber of the eye. Am J Hum Genet 68:364–372.

Ragge NK, Lorenz B, Schneider A, Bushby K, de Sanctis L, de Sanctis U, Salt A, Collin JR, Vivian AJ, Free SL, Thompson P, Williamson KA, Sisodiya SM, van Heyningen V, Fitzpatrick DR. 2005. SOX2 anophthalmia syndrome. Am J Med Genet Part A 135A:8.

Rao E, Weiss B, Fukami M, Rump A, Niesler B, Mertz A, Muroya K, Binder G, Kirsch S, Winkelmann M, Nordsiek G, Heinrich U, Breuning MH, Ranke MB, Rosenthal A, Ogata T, Rappold GA. 1997. Pseudoautosomal deletions encompassing a novel homeobox gene cause growth failure in idiopathic short stature and Turner syndrome. Nat Genet 16:54–63.

Rappold GA, Fukami M, Niesler B, Schiller S, Zumkeller W, Bettendorf M, Heinrich U, Vlachopapadoupoulou E, Reinehr T, Onigata K, Ogata T. 2002. Deletions of the homeobox gene SHOX (short stature homeobox) are an important cause of growth failure in children with short stature. J Clin Endocrinol Metab 87:1402–1406.

Schiller S, Spranger S, Schechinger B, Fukami M, Merker S, Drop SL, Troger J, Knoblauch H, Kunze J, Seidel J, Rappold GA. 2000. Phenotypic variation and genetic heterogeneity in Leri-Weill syndrome. Eur J Hum Genet 8:54–62.

Semina EV, Reiter R, Leysens NJ, Alward WL, Small KW, Datson NA, Siegel-Bartelt J, Bierke-Nelson D, Bitoun P, Zabel BU, Carey JC, Murray JC. 1996. Cloning and characterization of a novel bicoid-related homeobox transcription factor gene, RIEG, involved in Rieger syndrome. Nat Genet 14:392–399.

Semina EV, Ferrell RE, Mintz-Hittner HA, Bitoun P, Alward WL, Reiter RS, Funkhauser C, Daack-Hirsch S, Murray JC. 1998. A novel homeobox gene PITX3 is mutated in families with autosomal-dominant cataracts and ASMD. Nat Genet 19:167–170.

Semina EV, Brownell I, Mintz-Hittner HA, Murray JC, Jamrich M. 2001. Mutations in the human forkhead transcription factor FOXE3 associated with anterior segment ocular dysgenesis and cataracts. Hum Mol Genet 10:231–236.

Shears DJ, Vassal HJ, Goodman FR, Palmer RW, Reardon W, Superti-Furga A, Scambler PJ, Winter RM. 1998. Mutation and deletion of the pseudoautosomal gene SHOX cause Leri-Weill dyschondrosteosis. Nat Genet 19:70–73.

Stoilov I, Akarsu AN, Sarfarazi M. 1997. Identification of three different truncating mutations in cytochrome P4501B1 (CYP1B1) as the principal cause of primary congenital glaucoma (Buphthalmos) in families linked to the GLC3A locus on chromosome 2p21. Hum Mol Genet 6:641–647.

Stuppia L, Calabrese G, Gatta V, Pintor S, Morizio E, Fantasia D, Guanciali Franchi P, Rinaldi MM, Scarano G, Concolino D, Giannotti A, Petreschi F, Anzellotti MT, Pomilio M, Chiarelli F, Tumini S, Palka G. 2003. SHOX mutations detected by FISH and direct sequencing in patients with short stature. J Med Genet 40:E11.

Valleix S, Niel F, Nedelec B, Algros MP, Schwartz C, Delbosc B, Delpech M, Kantelip B. 2006. Homozygous nonsense mutation in the FOXE3 gene as a cause of congenital primary aphakia in humans. Am J Hum Genet 79:358–364.

Van Schoonveld MJ, Delleman JW, Beemer FA, Bleeker-Wagemakers EM. 1984. Peters'-plus: A new syndrome. Opphthal Paediatr Genet 4:141–145.

Woods KS, Cundall M, Turton J, Rizotti K, Mehta A, Palmer R, Wong J, Chong WK, Al-Zyoud M, El-Ali M, Otonkoski T, Martinez-Barbera JP, Thomas PQ, Robinson IC, Lovell-Badge R, Woodward KJ, Dattani MT. 2005. Over- and underdosage of SOX3 is associated with infundibular hypoplasia and hypopituitarism. Am J Hum Genet 76:833–849.